

High-resolution vessel wall magnetic resonance imaging for depicting imaging features of unruptured intracranial vertebrobasilar dissecting aneurysms

Binbin Sui^{1,2,3} , Xiaoyan Bai², Peiyi Gao^{2,3}, Yan Lin², Yisen Zhang⁴, Jia Liang² and Xinjian Yang⁴

Abstract

Objective: To demonstrate the application value of high-resolution vessel wall magnetic resonance imaging (HR-VW-MRI) for depicting the imaging features of unruptured intracranial vertebrobasilar dissecting aneurysms (VBDAs).

Methods: HR-VW-MRI data of 49 patients with suspected unruptured VBDAs were retrospectively analyzed. The presence of intramural hematomas (IMH), double lumens, intimal flaps, and outer diameter enlargements were recorded. Specificity and sensitivity were calculated for both two-dimensional (2D) and three-dimensional (3D) sequences. Additionally, IMH volumes were measured and posterior inferior cerebellar artery (PICA) involvement was analyzed.

Results: Thirty-five VBDAs were confirmed in 34 patients. The overall sensitivity and specificity were 0.889 (95% confidence interval [CI]: 0.730–0.964) and 0.769 (95% CI: 0.460–0.938) for 2D sequences, and 0.917 (95% CI: 0.764–0.978) and 0.846 (95% CI: 0.537–0.973) for 3D sequences, respectively. Intimal flaps were detected in 57.1%, 87.5%, and 71.4% of all cases on 2D pre-contrast T1-weighted, contrast-enhanced T1-weighted, and 3D T1-weighted black-blood (BB) images, respectively. There was no significant difference in IMH volume between 3D T1-weighted

¹Tiantan Neuroimaging Center of Excellence, China National Clinical Research Center for Neurological Diseases, Beijing, China

²Department of Radiology, Beijing Tiantan Hospital, Capital Medical University, Beijing Neurosurgical Institute, Beijing, China

³Beijing Key Laboratory of Magnetic Resonance Imaging and Brain Informatics, Beijing, China

⁴Department of Interventional Neurology, Beijing Tiantan Hospital, Capital Medical University, Beijing, China

Corresponding author:

Peiyi Gao, Beijing Tiantan Hospital, Capital Medical University, 119 West Road of South 4th Ring Road, Fengtai District, Beijing 100070, China.
Email: gaopeiyi20@126.com



BB and magnetization-prepared rapid gradient-echo sequences. PICA involvement was best visualized using 3D T1 sequences.

Conclusion: 3D T1-weighted BB MRI provided good visualization of VBDA features, with large coverage, and was useful for detecting dissection flaps.

Keywords

Vertebral artery dissection, basilar artery, magnetic resonance imaging, vessel wall imaging, high resolution, unruptured intracranial vertebrobasilar dissecting aneurysms, T1-weighted black-blood MRI

Date received: 6 April 2020; accepted: 4 November 2020

Introduction

Although spontaneous intracranial dissecting aneurysms (IDAs) are relatively rare, they are an important cause of stroke in young and middle-aged adults, and may have serious clinical consequences. These include ischemic stroke, transient ischemic attack, and subarachnoid hemorrhage.^{1,2} IDAs affect the posterior circulation more frequently than the anterior circulation, and the vertebral artery (intradural portion) is the most common site.³ East Asian populations are reported to have a higher incidence of intracranial aneurysms.⁴

IDA can be diagnosed by digital subtraction angiography (DSA), computed tomography angiography (CTA), and magnetic resonance angiography (MRA). The incidence of IDA may have increased recently because of developments in diagnostic technology. DSA remains the gold standard for the diagnosis of dissecting aneurysms; however, DSA is relatively limited for detecting vessel wall features, including intramural hematomas (IMHs). Multi-slice CTA is a sensitive and accurate technique for the diagnosis of arterial dissection. Previous research has demonstrated the high sensitivity (100%), specificity (98%), and accuracy (98.5%) of CTA for the detection of

extracranial vertebral artery dissections.⁵ Its high spatial resolution, fast imaging, and large coverage, as well as multiple post-processing techniques, allow CTA to provide good visualization of intracranial and extracranial arteries, with optimal performance in the detection of cervical arterial dissections.^{6,7} However, concerns include the radiation doses and the use of iodine contrast agents that are needed for this technique. Traditional magnetic resonance (MR) techniques, including routine MR imaging (MRI) and MRA, have a specificity of 29% to 100% and a sensitivity of 50% to 100% for detecting arterial dissections.⁸ In recent years, high-resolution (HR) vessel wall MRI (HR-VW-MRI) has been increasingly applied in clinical practice. This technique is an optimal and reliable method for visualizing intracranial vessel wall features.^{9,10}

Several black-blood (BB) techniques have been applied in vessel wall imaging. BB double inversion recovery and inflow saturation techniques have been widely used for two-dimensional (2D) imaging. Inversion recovery BB imaging can provide good spatial resolution and signal-to-noise contrast and has less flow artifacts, but it often has a relatively long acquisition time

compared with three-dimensional (3D) volumetric acquisition.

With the development of MR techniques, different 3D sequences have been applied for vessel wall imaging in recent years. 3D scanning sequences can be used to perform isotropic scanning, and can cover a large range in a relatively short time. Isotropic acquisition can improve through-plane resolution, and allows for vascular wall reconstruction in multiple planes. One of the most commonly used 3D vessel wall MR techniques involves 3D variable flip angle refocusing pulse fast spin-echo sequences, such as 3D volumetric isotropic turbo spin-echo acquisition (3D-VISTA),¹¹ 3D sampling perfection with application-optimized contrasts using different flip angle evolutions (3D-SPACE),¹² and 3D fast spin-echo with variable flip angle (CUBE)¹³ sequences. In contrast, 3D motion-sensitized driven-equilibrium rapid gradient echo (3D-MERGE)¹⁴ is based on a motion-sensitized driven-equilibrium (MSDE) preparation, which is a non-inflow-related technique. There are also sequences that are sensitive to subacute hemorrhage, including 3D magnetization-prepared rapid gradient-echo (3D MPRAGE) and simultaneous non-contrast angiography and intraplaque hemorrhage (SNAP) imaging.¹⁵ Previous studies have confirmed the high sensitivity and specificity of these two sequences for detecting IPHs.^{16,17} The application value of SNAP sequences for the screening of patients with suspected cervical dissection, and for the follow-up of IMHs after treatment, has also been reported.¹⁸

A previous study has demonstrated that HR-MRI can provide valuable information, such as about IMHs, in the diagnosis of IDAs. Moreover, this previous study revealed that some vessel wall imaging features are related to stroke occurrence in patients with cervicocranial artery dissection.¹⁹ However, 2D HR-MRI in clinical applications usually has a small imaging

scope, with a relatively long scanning time. There are clear limitations of 2D sequences when an IDA is large; in such cases, more time may be needed to obtain multi-contrast images. It is also hard for a 2D sequence to display multiple tortuous intracranial arteries in a cross-sectional plane with one acquisition. 3D fat-saturated T1-weighted (W) BB imaging has been applied in carotid dissection imaging with good image quality and application value,^{20,21} which indicates a possible diagnostic utility of this technique in IDAs.

In the present study, intracranial HR arterial wall imaging, including 3D T1W BB imaging, was performed in patients with suspected vertebrobasilar dissecting aneurysms (VBDAs) to investigate the application value of 3D T1W BB sequences for diagnosing VBDAs and demonstrating their characteristic features. This technique was also evaluated for its spatial coverage and scan time constraints, to explore its clinical relevance.

Methods

Study population

Between January 2014 and August 2016, we retrospectively reviewed data from patients with suspected unruptured intracranial VBDAs on 3D time-of-flight (TOF) MRA. Patients with previous intracranial stenting or embolization of the intracranial arteries, acute ischemic stroke, or MRI contraindications were excluded from this study. The study was approved by the institutional review board of Beijing Tiantan Hospital, Capital Medical University (approval no. KY2019-024-03), and written informed content was waived because of the retrospective nature of this study.

HR-MRI

MRI was performed using a MAGNETOM Trio, A Tim System 3T MR scanner

(Siemens Healthcare, Erlangen, Germany) with a 32-channel head coil. 3D TOF imaging was performed first, to define the location of the VBDA. HR-MRI included T2W turbo spin-echo (TSE), T1W TSE, MPRAGE, and 3D T1W SPACE sequences. Twenty-five cases also received contrast-enhanced (CE) T1W imaging. The HR-MRI parameters are listed in Table 1. 3D T1W SPACE was acquired in the oblique coronal plane, including the whole intracranial vertebrobasilar artery. Post-contrast T1W images were acquired 5 minutes after gadolinium injection (0.1 mmol/kg gadopentetate dimeglumine; Magnevist; Bayer HealthCare Pharmaceuticals, Berlin, Germany) using parameters identical to those of the pre-contrast T1W images.

Imaging evaluation

Two neuroradiologists (with 5 and 12 years, respectively, of experience in vascular neuroimaging) independently and blindly assessed the HR-MRI scans. A picture archiving and communication system (PACS) (DICOM 3.0, Neusoft, Shenyang, China) was used to visualize and evaluate

the cases, as well as to perform quantitative analyses. Multiplanar reconstructions were performed in the oblique sagittal and axial directions to visualize dissections from different planes for the 3D SPACE images (0.8-mm thickness, with no slice interval). The location and length of the dissection were recorded for each case. An IMH was defined as a false lumen filled with hematoma that displayed high signal on MPRAGE. Quantitative measurements of IMHs were performed manually using the PACS. A double lumen was noted when two lumens were displayed, with flow signal detected in both lumens. An intimal flap was identified as a linear layer across the lumen that extended to the arterial sidewall on any serial image. The signs of dissection, including IMH, double lumen, dissection flap, and maximum outer diameter of the involved artery, were recorded for both the 2D and 3D sequences. The posterior inferior cerebellar artery (PICA) involvement was also evaluated on 2D and 3D images. Discrepant findings between the two neuroradiologists were resolved by discussion. The final diagnosis was made by consensus among the

Table 1. Imaging parameters of magnetic resonance sequences.

Flow-suppression technique	3D TOF	T2W TSE	T1W TSE	MPRAGE	3D T1W SPACE Fat-saturated black blood Variable flip angle
	–	Inflow saturation	DIR	MSDE	
TR/TE (ms)	22/3.86	3000/65	750/12	776.13/5.8	800/22
TI (ms)	–	–	–	304	–
Flip angle (°)	25	180	180	20	–
Slice thickness (mm)	0.9	2.0	2.0	1.0	0.7
Number of slices	52	22	8	48	48
Field of view (mm)	160 × 160	160 × 160	160 × 160	180 × 180	240 × 160
Matrix	256 × 256	320 × 320	320 × 320	240 × 240	320 × 240
Scanning time	3'03"	3'23"	5'35"	3'29"	4'17"

3D, three-dimensional; TOF, time-of-flight; T2W, T2-weighted; TSE, turbo spin-echo; T1W, T1-weighted; MPRAGE, magnetization-prepared rapid gradient-echo; SPACE, sampling perfection with application-optimized contrasts using different flip angle evolutions; DIR, double inversion recovery; MSDE, motion-sensitized driven equilibrium; TR, repetition time; TE, echo time; TI, inversion time.

neuroradiologists, a neurointerventionist, and a neurologist, also combining evidence from clinical assessments and DSA scans.

Statistical analysis

Statistical analysis was performed using IBM SPSS Statistics for Windows, version 23.0 (IBM Corp., Armonk, NY, USA). Quantitative data are expressed as the mean \pm standard deviation. The one-sample Kolmogorov–Smirnov test was used to test the normality of data distribution. The paired-sample *t*-test and independent sample *t*-test were used for approximately normally distributed parameters. A value of $P < 0.05$ was considered statistically significant. The specificity and sensitivity were calculated for both 2D and 3D sequences. The intraclass correlation coefficient (ICC) was used to obtain the interobserver agreement for the IMH quantitative measurements between the two readers.

Results

*Diagnosis and location of the VBDA*s

In this study, 49 patients (41 male and 8 female patients, age range 18–82 years, median age 51 years) were included. Of these 49 patients, 34 were diagnosed with dissecting aneurysms. Of the other 15 patients, seven had flow artifacts, while eight had atherosclerotic plaques.

Thirty-five VBDA were identified in the 34 patients, with two lesions observed in one case. Eighteen VBDA were located at the right vertebral artery (RVA), nine at the left vertebral artery (LVA), and seven at the basilar artery (BA), while one VBDA involved both the BA and the LVA. In all 15 cases with a final diagnosis that excluded VBDA, nine were at the RVA, three at the LVA, and three at the BA.

Imaging findings of 2D axial HR-MRI

Most VBDA (33/35, 94.3%) presented as different degrees of outer-diameter enlargement on axial HR-MRI scans. The maximum outer diameter of all VBDA had an average value of 15.9 ± 8.2 mm (range 6–39 mm), whereas the average outer diameter of a normal adjacent vessel was 4.1 ± 1.2 mm (range 1.2–8.9 mm). There was a significant difference between the maximum outer diameter and the adjacent normal vessel diameter ($P < 0.001$). On MPRAGE sequences, IMHs were found in 60.0% (21/35) of cases, with an average volume of 4848.9 ± 10681.5 mm³ (range 55.1–36,191.9 mm³). Double lumens were observed in 85.7% (30/35) of cases, and dissection flaps were detected in 57.1% (20/35) of cases (Figure 1). Using CE T1W images, dissection flaps were identified in 16 of 18 cases (87.5%). The overall sensitivity and specificity for 2D axial HR-BB imaging sequences for intracranial VBDA diagnosis were 0.889 (95% CI: 0.730–0.964) and 0.769 (95% CI: 0.460–0.938), respectively. The positive and negative predictive values for 2D axial HR-BB imaging sequences for intracranial VBDA diagnosis were 0.914 (95% CI: 0.758–0.978) and 0.714 (95% CI: 0.420–0.904), respectively.

Imaging findings of 3D T1W BB images

For all cases, the 3D T1W BB sequence was able to cover the whole area of the vertebro-basilar arteries and all dissections. 3D T1W BB images were also able to detect all IMHs, with heterogeneous or homogeneous high signal displayed (Figure 2). The ICCs for IMH measurements were 0.973 (95% CI 0.931–0.989) for MPRAGE sequences and 0.891 (95% CI 0.741–0.957) for 3D T1W BB sequences. The average IMH volume on 3D T1W BB sequences was $2,938.3 \pm 6,019.5$ mm³ (range 21.6–22,260.5 mm³). Although the average IMH volume on 3D T1W BB sequences was lower than that on

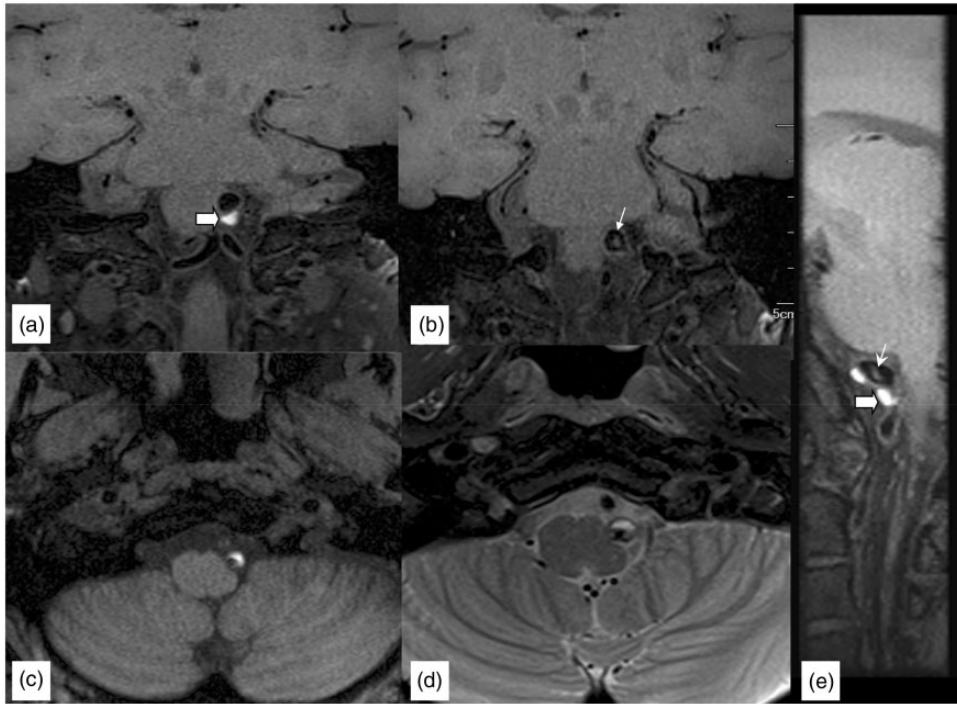


Figure 1. A 51-year-old woman with a dissection at the left vertebral artery (LVA). (a, b) Three-dimensional sampling perfection with application-optimized contrasts using different flip angle evolutions (3D SPACE) T1 images show an intramural hematoma (IMH; thick white arrow) and a dissection flap (small black arrow) in the lumen. (c) Magnetization-prepared rapid gradient-echo (MPRAGE) sequence detected the IMH, displaying high signal intensity at the LVA wall. (d) T2-weighted image showing high signal intensity of the vessel wall and low signal intensity of the lumen. (e) Oblique sagittal reformation of the 3D SPACE T1 image clearly shows the IMH (thick white arrow) and dissection flap (small white arrow).

MPRAGE, there was no significant difference in IMH volumes between 3D T1W BB and MPRAGE sequences ($P=0.113$). Double lumens were observed in 77.1% (27/35) of cases in the VBDA group using 3D T1W BB imaging. With multiplanar reconstruction²² and a thin slice thickness, dissection flaps were identified in 71.4% (25/35) of cases, which was higher than with T2WI (20/35). The overall sensitivity and specificity for 3D T1W BB sequences for intracranial VBDA diagnosis were 0.917 (95% CI: 0.764–0.978) and 0.846 (95% CI: 0.537–0.973), respectively. The positive and negative predictive values for 3D T1W BB sequences for VBDA diagnosis were 0.943

(95% CI: 0.794–0.990) and 0.786 (95% CI: 0.488–0.943), respectively.

Assessment of PICA involvement

PICA involvement was assessed in 3D TOF-MRA, T2W, and 3D SPACE images, respectively. There were 15 cases with PICA involvement. Of these, nine cases had right PICA involvement, five cases had left PICA involvement, and one case had bilateral PICA involvement. 3D SPACE displayed 29 cases of bilateral PICA, three cases of left PICA, and one case of right PICA. On 3D TOF-MRA images, 10 cases showed bilateral PICA, 12 cases showed left PICA, and seven

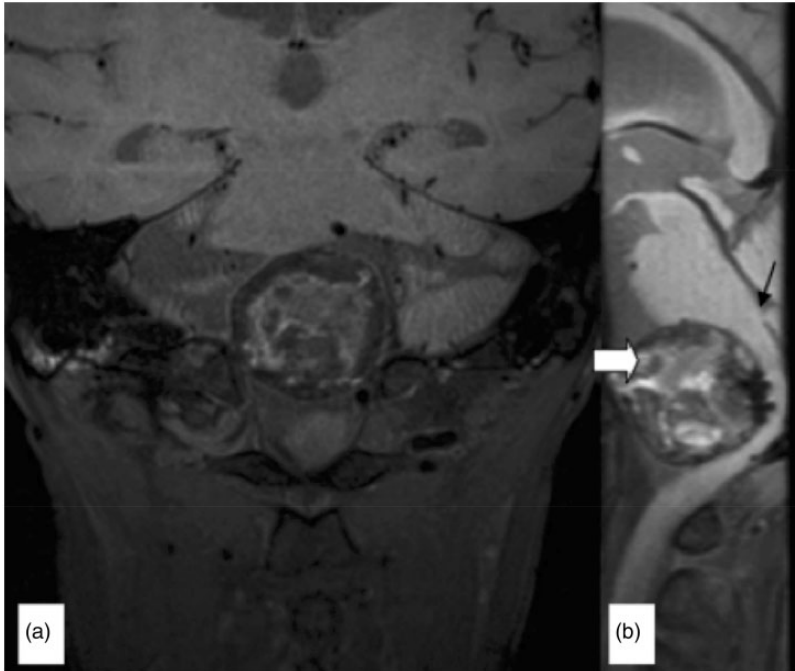


Figure 2. A 68-year-old man with a large dissecting aneurysm at the left vertebral artery (LVA). The outer diameter was obviously enlarged. (a, b) Heterogeneous signal intensity was observed in the lesion (thick white arrow), indicating intramural hematoma (IMH) and thrombosis of the dissecting aneurysm. The brainstem was obviously compressed (black arrow). The large coverage of three-dimensional sampling perfection with application-optimized contrasts using different flip angle evolutions (3D SPACE) T1 imaging allowed for better visualization of the lesion and adjacent structures.

cases showed right PICA. On T2W images, 19 cases showed bilateral PICA, four cases showed left PICA, and two cases showed right PICA (Figure 3). The visualization incidence of PICA involvement and other VBDA features on different MR sequences is displayed in Table 2.

Discussion

It is currently accepted that VBDA is more likely to represent a disease of the vessel wall than a disease of the vessel lumen. Therefore, imaging techniques that directly show the vessel wall structure can better demonstrate the characteristics of this lesion. The structures of the involved vessel wall and the classical features of

VBDA can be visualized well using HR-MRI techniques. Furthermore, it has been reported that different subtypes of spontaneous VBDA, with different imaging features, may be associated with a patient's clinical course.²³ Therefore, the accurate visualization of the imaging features of VBDA is very important for their clinical assessment. With high sampling efficiency and optimal blood suppression effects, 3D T1W BB imaging has been well accepted and applied in intracranial vessel imaging.^{10,24} It has also been demonstrated that 3D T1W BB imaging has a good performance in the diagnosis of VBDA.²⁵

The pathognomonic radiological findings of dissections include intimal flaps, double lumens, and IMHs. In the current

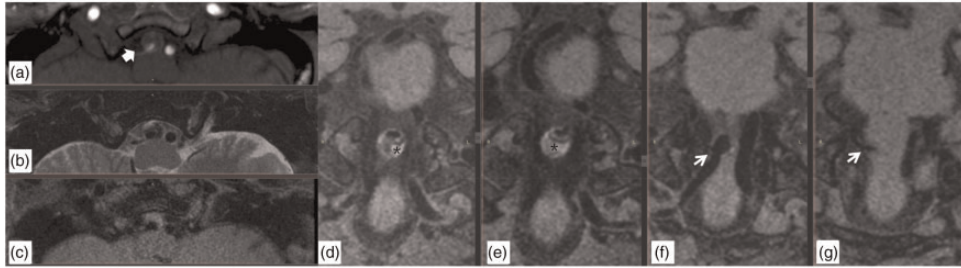


Figure 3. A 59-year-old man with a dissecting aneurysm at the right vertebral artery (RVA). The lesion shows (a) iso-low signal on time-of-flight magnetic resonance angiography (TOF MRA; thick white arrow), (b) heterogeneous low signal on two-dimensional (2D) axial T2-weighted imaging, and (c) slightly high signal on 2D axial T1-weighted imaging. (d–e) Three-dimensional (3D) T1-weighted black-blood (BB) images showing high signal intensity (*), indicating an intramural hematoma (IMH). (f–g) 3D T1-weighted BB images at another two sequential slices showing the origin and path of the right posterior inferior cerebellar artery (PICA; white arrow).

Table 2. Detection performances of various features of vertebrobasilar dissecting aneurysms for high-resolution magnetic resonance sequences.

Sequences/VBDA features	Intramural hematoma	Double lumen	Dissection intimal flap	PICA involvement
2D T2W TSE	–	57.1% (20/35)	57.1% (20/35)	80% (12/15)
2D T1W TSE	90.4% (19/21)	34.3% (12/35)	25.7% (9/35)	–
3D TOF MRA	71.4% (15/21)	45.7% (16/35)	22.8% (6/35)	53.3% (8/15)
3D MPRAGE	100% (21/21)	–	–	–
3D T1W SPACE	100% (21/21)	77.1% (27/35)	71.4% (25/35)	86.6% (13/15)
2D CE T1W	–	87.5% (16/18)	87.5% (16/18)	–

VBDA, vertebrobasilar dissecting aneurysm; PICA, posterior inferior cerebellar artery; 2D, two-dimensional; T2W, T2-weighted; TSE, turbo spin-echo; T1W, T1-weighted; 3D, three-dimensional; TOF, time-of-flight; MRA, magnetic resonance angiography; MPRAGE, magnetization-prepared rapid gradient-echo; SPACE, sampling perfection with application-optimized contrasts using different flip angle evolutions; CE, contrast-enhanced.

study, 3D T1W BB imaging offered several advantages for detecting the features of VBDA compared with 2D axial imaging. With 3D acquisition in submillimetric, and almost isotropic, voxels ($0.7 \times 0.7 \times 0.7$ mm in our study), multiplanar reconstruction allowed observations from different angles with good image quality. This technique provided better visualization of the imaging characteristics of dissecting aneurysms compared with 2D T1W TSE imaging.

An IMH is an important feature, displaying as a change in the vessel wall, that can be missed using DSA and CTA. It has

been reported that a persistent high signal intensity of IMHs in VBDA after reconstructive endovascular treatment may be associated with the progression of VBDA.²⁶ In our dataset, 3D T1W BB imaging was able to visualize all IMHs. Although there was no significant difference in IMH volume between 3D T1W SPACE and MPRAGE, the IMH volumes on MPRAGE were larger than those on SPACE. This finding may be caused by differences in the principles of these two sequences. The ICC results revealed that interobserver agreement was good for

both of these sequences. The thin slice thickness (0.7 mm) in 3D T1W BB imaging may help to display some small IMHs, which might be important for the dissection diagnosis.

For intracranial arteries, vessel structure is relatively small; therefore, intimal flaps may be hard to identify. In the present study, the use of 3D T1W BB sequences also increased the detection of dissection flaps compared with 2D axial images. A previous study reported that dissection flaps were able to be detected in 91.4% of cases using CE T1WI, and 68.6% of cases using T2WI.²⁷ In the current study, the incidence was 57.1% (20/35) using T2WI and 87.5% (16/18) using CE T1WI. When using SPACE, the detection incidence was 71.4% (25/35). The multiplanar reconstruction of SPACE has the advantage of allowing observations from different projections because of its thin slice thickness; this is better for the detection of intimal flaps. Because intimal flaps were better visualized in CE images, post-contrast 3D SPACE images may be even more useful for the diagnosis of dissection diseases.

Another advantage of SPACE sequences is the large field of view in the z-axis. It can take a relatively long time to cover the whole lesion for large dissecting aneurysms. For intracranial imaging, the oblique coronal acquisition of the SPACE sequence can cover the whole intracranial segment of the vertebral and basilar arteries within a relatively short acquisition time, which is useful for VBDA that involve long vessel segments. With a shorter acquisition time, of 4 minutes 17 s versus 5 minutes 35 s for a 2D T1W TSE dark blood sequence, the 3D T1W SPACE sequence was able to cover the whole intracranial segment of the vertebral and basilar arteries.

PICA involvement is an important factor for the management of VBDA. T2WI provides good contrast for the assessment of PICA involvement. One study has reported

that T2W HR-VW-MRI can clearly display arterial shape changes in PICA dissections.²⁸ However, in seven cases from the VBDA group, PICA was unable to be visualized on T2WI because of the limited coverage in this group. In contrast, 3D T1W BB imaging was able to detect most of the PICA involvement in this group, with its large coverage area. The failure of 3D T1W BB imaging to display PICA was mainly caused by signal loss near the rim of the coil or slab. Signal loss near the edge of the acquisition slab is common in 3D protocols. The slab thickness should therefore be set carefully to be larger than the region of interest. In summary, 3D T2W BB sequences with good signal-to-noise ratio and contrast might be useful for the evaluation of PICA involvement in VBDA.

The sensitivity and specificity of the 3D BB sequence were higher than those of the 2D sequence. However, both sequences showed excellent sensitivity with good specificity. In contrast, the negative predictive values for both the 2D and 3D sequences were relatively low. In some cases, flow artifact can resemble an intimal flap, which may cause false-positive detections. Recently, a study using the delay alternating with nutation for tailored excitation (DANTE) preparation module incorporated into SPACE was able to demonstrate improved arterial and venous blood suppression compared with SPACE alone.²⁹ The application of this new technique may further improve the diagnosis and post-surgical monitoring of VBDA. Based on the findings of the present study, we suggest that the optimal protocol for IAD includes pre- and post-3D T1W BB imaging, MPRAGE, and 2D axial T2W BB imaging, while 3D T2W BB imaging can be an alternative sequence.

This work is subject to some limitations. For example, the sample size of this study was relatively small. There were also limitations in the quantitative assessment of

IMHs in this study. For large dissecting aneurysms that include both IMH and thrombosis, it is difficult to differentiate the IMH from the thrombosis and to accurately measure the IMH in the aneurysm. Another limitation to the present study was that not all patients accepted CE imaging, which displayed more features of VBDA. Post-contrast 3D T1W BB imaging is useful for VBDA diagnosis, and wall enhancement on HR-MRI was also demonstrated to be related to the progression of VBDA after reconstructive endovascular treatment.³⁰ The post-contrast sequence, including post-contrast 3D T1W BB imaging, should be applied in further studies.

In conclusion, HR-VW-MRI allows the good visualization of VBDA features. 3D T1W BB imaging is superior to 2D axial sequences, with its large coverage area and thin slice thickness. Multiplanar reconstruction of 3D source images may help to detect dissection flaps.

Acknowledgement

The authors are thankful to Tianyi Qian for his help with MR sequence adjustment and manuscript revision.

Declaration of conflicting interest

The authors declare that there is no conflict of interest.

Funding

This work was supported by the National Natural Science Foundation of China (grant no. 81301193, 81801158), National Key Research and Development Project of China (2018YFC1312004), and the Beijing Municipal Health System High Level Medical Personnel Discipline Backbone Project (2015-3-037).

ORCID iD

Binbin Sui  <https://orcid.org/0000-0002-1052-6992>

References

1. Mizutani T, Aruga T, Kirino T, et al. Recurrent subarachnoid hemorrhage from untreated ruptured vertebrobasilar dissecting aneurysms. *Neurosurgery* 1995; 36: 905–911.
2. Arnold M, Boussier MG, Fahrni G, et al. Vertebral artery dissection: presenting findings and predictors of outcome. *Stroke* 2006; 37: 2499–2503.
3. Debette S, Compter A, Labeyrie MA, et al. Epidemiology, pathophysiology, diagnosis, and management of intracranial artery dissection. *Lancet Neurol* 2015; 14: 640–654.
4. Tsukahara T and Minematsu K. Overview of spontaneous cervicocephalic arterial dissection in Japan. *Acta Neurochir Suppl* 2010; 107: 35–40.
5. Chen CJ, Tseng YC, Lee TH, et al. Multisection CT angiography compared with catheter angiography in diagnosing vertebral artery dissection. *AJNR Am J Neuroradiol* 2004; 25: 769–774.
6. Hanning U, Sporns PB, Schmiedel M, et al. CT versus MR techniques in the detection of cervical artery dissection. *J Neuroimaging* 2017; 27: 607–612.
7. Sporns PB, Niederstadt T, Heindel W, et al. Imaging of spontaneous and traumatic cervical artery dissection: comparison of typical CT angiographic features. *Clin Neuroradiol* 2019; 29: 269–275.
8. Provenzale JM and Sarikaya B. Comparison of test performance characteristics of MRI, MR angiography, and CT angiography in the diagnosis of carotid and vertebral artery dissection: a review of the medical literature. *AJR Am J Roentgenol* 2009; 193: 1167–1174.
9. Alexander MD, Yuan C, Rutman A, et al. High-resolution intracranial vessel wall imaging: imaging beyond the lumen. *J Neurol Neurosurg Psychiatry* 2016; 87: 589–597.
10. Mandell DM, Mossa-Basha M, Qiao Y, et al. Intracranial vessel wall MRI: principles and expert consensus recommendations of the American Society of Neuroradiology. *AJNR Am J Neuroradiol* 2017; 38: 218–229.
11. Qiao Y, Steinman DA, Qin Q, et al. Intracranial arterial wall imaging using three-dimensional high isotropic resolution black blood MRI at 3.0 Tesla. *J Magn Reson Imaging* 2011; 34: 22–30.

12. Zhang L, Zhang N, Wu J, et al. High resolution three dimensional intracranial arterial wall imaging at 3 T using T1 weighted SPACE. *Magn Reson Imaging* 2015; 33: 1026–1034.
13. Li ML, Xu YY, Hou B, et al. High-resolution intracranial vessel wall imaging using 3D CUBE T1 weighted sequence. *Eur J Radiol* 2016; 85: 803–807.
14. Makhijani MK, Balu N, Yamada K, et al. Accelerated 3D MERGE carotid imaging using compressed sensing with a hidden Markov tree model. *J Magn Reson Imaging* 2012; 36: 1194–1202.
15. Wang J, Guan M, Yamada K, et al. In vivo validation of simultaneous non-contrast angiography and intraplaque hemorrhage (SNAP) magnetic resonance angiography: an intracranial artery study. *PLoS One* 2016; 11: e0149130.
16. Ota H, Yarnykh VL, Ferguson MS, et al. Carotid intraplaque hemorrhage imaging at 3.0-T MR imaging: comparison of the diagnostic performance of three T1-weighted sequences. *Radiology* 2010; 254: 551–563.
17. Li D, Zhao H, Chen X, et al. Identification of intraplaque haemorrhage in carotid artery by simultaneous non-contrast angiography and intraplaque haemorrhage (SNAP) imaging: a magnetic resonance vessel wall imaging study. *Eur Radiol* 2018; 28: 1681–1686.
18. Huang RJ, Lu Y, Zhu M, et al. Simultaneous non-contrast angiography and intraplaque haemorrhage (SNAP) imaging for cervical artery dissections. *Clin Radiol* 2019; 74: 817.e1–817.e7.
19. Wu Y, Wu F, Liu Y, et al. High-resolution magnetic resonance imaging of cervicocranial artery dissection: imaging features associated with stroke. *Stroke* 2019; 50: 3101–3107.
20. Cuvinciu V, Viallon M, Momjian-Mayor I, et al. 3D fat-saturated T1 SPACE sequence for the diagnosis of cervical artery dissection. *Neuroradiology* 2013; 55: 595–602.
21. Luo Y, Guo ZN, Niu PP, et al. 3D T1-weighted black blood sequence at 3.0 Tesla for the diagnosis of cervical artery dissection. *Stroke Vasc Neurol* 2016; 1: 140–146.
22. Iampreechakul P, Tanpun A, Lertbusayanukul P, et al. Contralateral extensive cerebral hemorrhagic venous infarction caused by retrograde venous reflux into the opposite basal vein of Rosenthal in posttraumatic carotid-cavernous fistula: a case report and literature review. *Interv Neuroradiol* 2018; 24: 546–558.
23. Zhang Y, Tian Z, Sui B, et al. Endovascular treatment of spontaneous intracranial fusiform and dissecting aneurysms: outcomes related to imaging classification of 309 cases. *World Neurosurg* 2017; 98: 444–455.
24. Zhu C, Haraldsson H, Tian B, et al. High resolution imaging of the intracranial vessel wall at 3 and 7 T using 3D fast spin echo MRI. *Magma* 2016; 29: 559–570.
25. Choi JW, Han M, Hong JM, et al. Feasibility of improved motion-sensitized driven-equilibrium (iMSDE) prepared 3D T1-weighted imaging in the diagnosis of vertebrobasilar artery dissection. *J Neuroradiol* 2018; 45: 186–191.
26. Tian Z, Chen J, Zhang Y, et al. Quantitative analysis of intracranial vertebrobasilar dissecting aneurysm with intramural hematoma after endovascular treatment using 3-T high-resolution magnetic resonance imaging. *World Neurosurg* 2017; 108: 236–243.
27. Han M, Rim NJ, Lee JS, et al. Feasibility of high-resolution MR imaging for the diagnosis of intracranial vertebrobasilar artery dissection. *Eur Radiol* 2014; 24: 3017–3024.
28. Madokoro Y, Sakurai K, Kato D, et al. Utility of T1- and T2-weighted high-resolution vessel wall imaging for the diagnosis and follow up of isolated posterior inferior cerebellar artery dissection with ischemic stroke: report of 4 cases and review of the literature. *J Stroke Cerebrovasc Dis* 2017; 26: 2645–2651.
29. Xie Y, Yang Q, Xie G, et al. Improved black-blood imaging using DANTE-SPACE for simultaneous carotid and intracranial vessel wall evaluation. *Magn Reson Med* 2016; 75: 2286–2294.
30. Zhang Y, Sui B, Liu J, et al. Aneurysm wall enhancement on magnetic resonance imaging as a risk factor for progression of unruptured vertebrobasilar dissecting aneurysms after reconstructive endovascular treatment. *J Neurosurg* 2018; 128: 747–755.